UNIVERSIDAD DE CHILE
FACULTAD DE CIENCIAS FÍSICAS Y MATEMÁTICAS
DEPARTAMENTO DE INGENIERIA DE MINAS

EVALUATION OF SEISMIC ROCK MASS RESPONSE TO MINING USING A STOCHASTIC MODEL OF THE EPIDEMIC TYPE

TESIS PARA OPTAR AL GRADO DE MAGISTER EN MINERÍA

FEDILBERTO JOSÉ GONZALEZ ARIAS

PROFESOR GUÍA:
JAVIER VALLEJOS MASSA

PROFESOR CO-GUIA
RAUL CASTRO RUIZ

MIEMBROS DE COMISIÓN
KIMIE SUZUKI MORALES
DMITRIY MALOVICHKO

SANTIAGO DE CHILE
2019

RESUMEN

Con la profundización de las actividades mineras, los ambientes de alto esfuerzo se han vuelto más comunes en los últimos años. Estos ambientes implican un aumento del peligro sísmico generado por la ocurrencia de rockburst. Actualmente, minas propensas a rockburst suelen realizar un análisis demasiado simplista de los datos sísmicos registrados. Por lo tanto, para proporcionar un análisis avanzado de la sismicidad registrada, el modelo estocástico Epidemic Type Aftershock Sequences (ETAS) fue propuesto. El modelo ETAS ha sido implementado extensivamente en sismología global en los últimos 30 años para la detección de quiescencia relativa precursora antes de grandes terremotos. Este modelo simula un proceso en el que cada evento produce sus propios eventos descendientes, introduciendo el concepto de sismicidad "inducida".

A partir de la diferencia entre la sismicidad medida y la estimada con el modelo (análisis residual), se ilustran varias alertas sísmicas en calibración y aplicación. El análisis residual presentó valores de parámetros críticos más grandes que precedieron a algunos de los eventos sísmicos de gran magnitud. Considerando que las actividades extractivas, explosiones y cambios litológicos no son continuos en el espacio o en el tiempo, se espera que el número de falsas alarmas tienda a aumentar con el tiempo cuando la respuesta sísmica de la roca excede las desviaciones estándar preestablecidas (Esta investigación utilizó $\sigma = 1.5$). Además, se percibe cómo el modelo ETAS a través del análisis residual muestra los niveles sísmicos en la extensión del túnel en presencia de tres cuerpos hidrotermales A, B y C, lo que permite comprender la respuesta del macizo rocoso a los cambios litológicos. Finalmente, se proponen algunos gráficos auxiliares para mejorar la comprensión del comportamiento del residual.

Los parámetros del modelo ETAS se ven afectados por el proceso minero. Se recomienda utilizar el período de mejor ajuste de los registros para calibrar los parámetros. Por lo tanto, se sugiere dividir el período analizado en segmentos de acuerdo con el Criterio de Información de Akaike. Para ayudar a implementar el modelo ETAS en el futuro, se discute la calibración, evaluación y aplicación de parámetros basados en el análisis de la sismicidad registrada para el túnel de ventilación (XC22/23) en la mina El Teniente. Los resultados de la implementación del modelo ETAS en un periodo futuro fueron satisfactorios, el valor AIC en la calibración fue similar al valor AIC en la aplicación.

ABSTRACT

With the depth of mining activities, high-stress environments have become more prevalent in recent years. These environments imply an increase in the seismic hazard generated by the occurrence of rockburst. Actually, modern rockburst-prone mines tend to perform an often too simplistic analysis of recorded seismic data. Therefore, to provide an advanced analysis of recorded seismicity, the stochastic Epidemic Type Aftershock Sequences (ETAS) model was proposed. The ETAS model has been extensively implemented in global seismology over the last 30 years for the detection of precursory relative quiescence before great earthquakes. This model simulates a process in which each event produces its own offspring events, introducing the concept of "induced" seismicity.

Based on the difference between the measured seismicity and that estimated using the model (residual analysis), several seismic alerts in calibration and application are illustrated. The residual analysis presented larger critical parameter values preceding some of the largest-magnitude seismic events. Considering that extractive activities, blasts, and lithological changes are not continuous in space or time, it is expected that the number of false alarms tends to increase with time when the seismic response of the rock exceeds the pre-established standard deviations (This research used $\sigma = 1.5$). Also, it is perceived how the ETAS model through the residual analysis exhibits the seismic levels in the extension of the tunnel in the presence of three hydrothermal bodies A, B, and C, providing an understanding of the rock mass response to lithological changes. Finally, some auxiliary graphs are proposed to improve the understanding of the behavior of residuals.

The parameters of the ETAS model are affected by the mining process. The use of the best-fit period of records to calibrate the parameters is recommended. Therefore, dividing the period analyzed into segments according to the Akaike Information Criterion is suggested. To help the implementation of the ETAS model in the future, calibration, evaluation, and application of parameters are discussed based on the analysis of recorded seismicity for the ventilation tunnel (XC22/23) at the El Teniente mine. The results of implementing the ETAS model to a future period were satisfactory, the AIC value in the calibration was similar to AIC value in the application.

TABLE OF CONTENTS

LIST OF FIGURES

LIST OF TABLES

1. INTRODUCCION

La modernización de las actividades mineras ha ocasionado que se invierta una cantidad importante de recursos para evaluar el peligro sísmico a través de modelos empíricos y numéricos. La inevitable expansión en profundidad de las actividades mineras para mantener o aumentar su productividad, ocasiona un aumento de dicho peligro en el tiempo. En zonas con un mayor peligro sísmico asociado, se podría esperar una liberación más violenta de deformación inelástica dentro de un tamaño de roca. Cuando esta liberación causa daños sobre la apertura de una mina, es denominado “rockburst” (Kaiser et al., 1996). Aunque en la actualidad no hay una definición globalmente aceptada sobre este fenómeno complejo, como es aclamado por Suorineni et al., (2014), los rockbursts son el “cáncer” de la minería (Zhou, et al., 2017). En esta investigación, rockbursts se definen como los eventos sísmicos con magnitud de momento Hanks-Kanamori $M_W \geq 0.7$.

Implementando la sismicidad registrada durante el desarrollo del túnel de ventilación XC22/23 en la mina El Teniente, esta investigación postula el uso del modelo estocástico ETAS (Epidemic Type Aftershock Sequences) para la estimación del peligro sísmico y la tasa esperada de eventos sísmicos. Basado en las agrupaciones sísmicas en espacio, tiempo y magnitud de cada evento sísmico registrado, este modelo simula un proceso en el que cada evento produce sus propios eventos descendientes (Ogata 1983; 1985; 1988; 1989). Es decir, el modelo ETAS incorpora la noción de sismicidad "inducida".

El modelo ETAS fue utilizado por primera vez en minería para estimar el peligro sísmico en minas de Canadá y Australia (Trifu y Shumila, 2005). Para complementar el enfoque anterior, esta investigación ilustra varias alertas sísmicas en calibración y aplicación a partir de la diferencia entre la sismicidad medida y la estimada mediante el modelo (análisis residual). Para hacer más riguroso el análisis, los cuerpos hidrotermales identificados por geología fueron introducidos en los gráficos que exhiben el análisis residual. Adicionalmente, una serie de gráficos auxiliares fueron propuestos para justificar el comportamiento del residual. Las modificaciones al modelo ETAS convencional fueron sugeridas debido al comportamiento dinámico de la sismicidad en minería.

Los parámetros del modelo ETAS permiten un amplio conocimiento sobre el nivel sísmico de fondo, velocidad de decaimiento y el peligro sísmico de una amplia zona de interés. Estos parámetros se relacionan con las perturbaciones del proceso minero. Para calibrar los parámetros, se recomienda utilizar el período de tiempo más adecuado en los registros disponibles. Por lo tanto, utilizando el criterio de información de Akaike, se evalúan los posibles cambios paramétricos en los periodos analizados. La versatilidad del modelo ETAS tiene potencial para hacerlo ampliamente aplicable en la minería.

1.1. ESTADO DE ARTE

El modelo ETAS simula un proceso en el que cada evento produce su propia secuencia de eventos. Este modelo fue introducido por Ogata (1988; 1992) en la sismología. Sin embargo, el modelo epidémico original, llamado proceso de "nacimiento y muerte", fue considerado por Kendall (1949). Posteriormente, Hawkes (1971) implementó el proceso de intensidad condicional basado en la historia de los tiempos de ocurrencia. Desde el trabajo pionero de Omori (1894), algunos autores han estudiado extensamente el aspecto de las actividades sísmicas como Utsu y Seki (1955), Utsu (1957; 1961; 1962) y Mogi (1967). Inspirado por estos autores, Ogata (1983; 1985; 1988; 1989) sugirió modelos estadísticos que permiten estimar el número esperado de réplicas sísmicas de terremotos en secuencias estandarizadas de una zona de interés. Ogata (1992) utilizó la observación ampliamente difundida de que antes de un gran terremoto había una quiescencia sísmica previa y luego una actividad premonitoria (foreshocks) para validar el uso del modelo ETAS para dar alertas sísmicas. Inouye (1965), Utsu (1968) y Mogi (1968) estudiaron la quiescencia para predecir terremotos. El actual modelo ETAS es especialmente útil cuando la identificación de los eventos principales o réplicas no es fácil. Con el análisis de sismicidad ordinario, este enfoque no es posible.

Como fue discutido por Kijko (1966), es posible modelar el peligro sísmico en minería mediante la implementación de réplicas sísmicas. Basándose en este enfoque, Trifu y Shumila (2005) propusieron

estimar el peligro sísmico utilizando el modelo ETAS. Con el análisis residual, fue posible seguir la respuesta del macizo rocoso en períodos de calibración con base en el análisis de la sismicidad registrada para el túnel de ventilación (XC22/23) en la mina El Teniente.

1.2. PREAMBULO

Los problemas asociados a los eventos de rockbursts de la mina El Teniente, fueron publicados por primera vez por la Sociedad Nacional de Minería de Chile en mayo de 1990 (Sociedad Nacional de Minería, 1990). Estos eventos sísmicos causaron pérdidas de personal, daños a los equipos y una disminución de 20,000 tpd en la productividad de la mina. Luego, en 1994, comenzó una fase de estudio llamada "Minería Experimental". En este contexto, numerosos investigadores y consultores de todo el mundo intentaron comprender, mitigar y prevenir el daño máximo de los eventos de rockburst, implementando modelos empíricos y numéricos. El número de rockbursts comenzó a disminuir desde 2005 con la introducción de la técnica de fracturamiento hidráulico (Rojas & Balboa, 2017). Antes de su aplicación en el túnel XC22/23, el fracturamiento hidráulico (FH) en la mina El Teniente se centraba en mitigar el peligro sísmico durante los procesos de caving. Por lo tanto, el primer diseño de FH a "escala de túnel" se realizó con una línea de pozos a lo largo del eje del túnel XC22/23 (Rojas & Landeros, 2017).

1.3. MOTIVACION

A medida que las actividades mineras se han ido profundizando, los problemas relacionados con la sismicidad inducida son cada vez más una realidad. En el caso de Chile, en donde el esfuerzo horizontal está condicionado fuertemente por la subducción, condiciones de altos esfuerzos pueden ser alcanzados a menor profundidad.

El fenómeno de la sismicidad inducida está siendo ampliamente estudiado en países cuya minería se encuentra entre los 1500- 4000 [m] de profundidad como es el caso de Sudáfrica, Canadá y Australia. Las condiciones geológicas chilenas, en combinación con las profundidades alcanzadas de sus minas, crean una necesidad en la investigación y aporte científico sobre el fenómeno de la sismicidad inducida.

1.4. OBJETIVOS

El objetivo principal de esta investigación es la calibración, evaluación y aplicación del modelo ETAS utilizando la sismicidad inducida registrada en el túnel (XC22/23) en la mina El Teniente. Además, utilizar el análisis residual para seguir la respuesta sísmica del macizo rocoso a la minería aplicada y dar algunas alertas sísmicas cuando sea posible.

1.5. ALCANCES DEL ESTUDIO

1. Usar la sismicidad inducida registrada en el túnel (XC22/23) en la mina El Teniente.
2. Las alertas sísmicas identificadas con el modelo ETAS tienen magnitud de momento Hanks-Kanamori $M_W \geq 0.7$.

1.6. METODOLOGIA

Para lograr los objetivos planteados, es necesario:

1. La identificación de los cuerpos hidrotermales y su ocurrencia en el espacio-tiempo específico.
2. Calibración de los parámetros del modelo ETAS.
3. División del período analizado en segmentos según el Criterio de Información de Akaike (AIC).
4. Uso del análisis residual para seguir la respuesta del macizo rocoso a la minería aplicada.

1.7. RESUMEN DE LA INVESTIGACION

Esta investigación fue presentada en los siguientes artículos:

Art.1: "Evaluation of the Seismic Response of the Rock Mass Using a Model of Seismic Aftershocks of the Epidemic Type"

Los primeros resultados de esta investigación fueron presentados en el simposio ARMA (American Rock Mechanics Association). Véase la referencia al artículo a continuación:

Gonzalez, F. J., and J. A. Vallejos. "Evaluation of the Seismic Response of the Rock Mass Using a Model of Seismic Aftershocks of the Epidemic Type" *53rd US Rock Mechanics/Geomechanics Symposium*. American Rock Mechanics Association, 2019.

Art.2: "Methodology for the Seismic Alerts Standardization in Mining Using a Stochastic Model of Seismic Aftershocks"

Centrándose en el posible uso del modelo ETAS en tiempo real, se implementaron algunas mejoras. Una versión actualizada del modelo ETAS fue publicada en el 14º Congreso Internacional ISRM (International Society for Rock Mechanics). Véase la referencia al artículo a continuación:

Gonzalez, F. J., and J. A. Vallejos. " Methodology for the Seismic Alerts Standardization in Mining Using a Stochastic Model of Seismic Aftershocks". *Proceedings of the 14th International Congress on Rock Mechanics and Rock Engineering (ISRM 2019), September 13-18, 2019, Foz do Iguassu, Brazil*.

Los dos artículos mencionados anteriormente tienen un contenido similar. Por lo tanto, este documento sólo incluirá el resumen del articulo enviado al simposio ARMA y el contenido completo enviado al Congreso Internacional ISRM.

1.8. BIBLIGORAFIAS

Hawkes, A.G. (1971). Point spectra of some mutually exciting point processes, J. R. Statist. Soc., Set. B, 33, 438-443.

Inouye, W. (1965). On the seismicity in the epicentral región and its neighborhood before the Niigata earthquake, (in Japanese), Kenshin-jiho (Q. J. Seismol.), 29, 139-144.

Kaiser, P.K., Tannant, D.D., McCreath, D.R., 1996. Canadian Rockburst Support Handbook. Geomechanics Research Centre, Laurentian University, Sudbury, Ontario, pp. 314

Kendall, D.G. (1949). Stochasticp rocesses and population grouth, J. R. Statist. Soc., Set. B, 11, 230-264.

Kijko A (1996) Statistical method in minin seismology. South African Geophys. Assoc., Johannesburg.

Mogi, K.(1968). Some features of recent seismic activity in and near Japan (1), Bull. Earthquake Res. Inst., Univ. Tokyo, •6, 1225-1235.

Ogata Y (1983). Likelihood analysis of point processes and its application to seismological data. Bull Int Stat Inst 50:943–961.

Ogata, Y.(1985). Statistical models for earthquake occurrences and residual análisis for point processes, Res. Memo. (Technical report) 288, Inst. Statist. Math., Tokyo.

Ogata Y. (1988). Statistical Models for Earthquake Occurrences and Residual Analysis for Point Processes. J Am Stat Assoc 83:9–27. https://doi.org/10.1080/01621459.1988.10478560.

Ogata Y. (1989). Statistical model for standard seismicity and detection of anomalies by residual analysis. Tectonophysics 169:159–174. https://doi.org/10.1016/0040-1951(89)90191-1.

Ogata Y. (1992). Detection of precursory relative quiescence before great earthquakes through a statistical model. J Geophys Res 97:19845. https://doi.org/10.1029/92jb00708.

Omori, F. (1894). On the after-shocks of earthquakes. The Journal of the College of Science, Imperial University of Tokyo, 7, 111-200.

Rojas E, Balboa S (2017) Management of seismic risk in high stress conditions, El Teniente mine. In: The 9th Rockburst and Seismicity in Mines Symposium (RaSIM 9)

Rojas E, Landeros P (2017) Hydraulic fracturing applied to tunnels development at El Teniente mine. In: The 9th Rockburst and Seismicity in Mines Symposium (RaSIM 9).

Sociedad Nacional de Minería. (1990). Explosiones de Rocas en El Teniente (ISSN-0378-0961, Año CIV N° 47). Recuperado de: http://www.bibliotecanacionaldigital.gob.cl/colecciones/BND/00/RE/RE0000545_0048.

Suorineni, F.T., Hebblewhite, B., Saydam, S., 2014. Geomechanics challenges of contemporary deep mining: a suggested model for increasing future mining safety and productivity. JS Afr. Inst. Min. Metall. 114 (12), 1023–1032.

Trifu, C., & Shumila, V. (2005). Seismic hazard assessment in mines using a marked spatio-temporal point process model. Controlling Seismic Risk (Eds. Potvin, Y., and Hudyma, M.), Australian Centre for Geomechanics, Perth, Australia, 461–467.

Utsu, T., and A. Seki. (1955). Relation between the area of aftershock region and the energy of the main shock (in Japanese), Zisin (J. Seismol. Soc. Japan), 2nd Ser., ii,7 233-40.

Utsu, T. (1957). Magnitude of earthquakes and occurrence of their aftershocks, (in Japanese), Zisin (J. Seismol. Soc. Jap.) ii 10, 35-45.

Utsu, T.(1961). A statistical study on the occurrence of aftershocks, Geophys. Mag., 30, 521-605.

Utsu, T. (1962). On the nature of three Alaskan aftershock sequences, Bull. Seismol. Soc. Am., 52, 279-297.

Utsu, T. (1968). Seismic activity in Hokkaido and its vicinity (in Japanese), Geophys. Bull. Hokkaido Univ., 13, 99-103.

Zhou, Jian, Xibing Li, and Hani S. Mitri. "Evaluation method of rockburst: state-of-the-art literature review." *Tunnelling and Underground Space Technology* 81 (2018): 632-659.

2. Evaluation of the Seismic Response of the Rock Mass Using a Model of Seismic Aftershocks of the Epidemic Type

Fedilberto Gonzalez[a], Javier Vallejos[a,b]

[a] Advanced Mining Technology Center, University of Chile, Santiago, Chile

[b] Department of Mining Engineering, University of Chile, Santiago, Chile

Keywords: rockbursts, ETAS, offspring events.

2.1. ABSTRACT

High-stress environments have become more common in recent years as mines are getting deeper every time. These environments imply an increase in the seismic hazard generated by the sudden release of energy from mining activities. Seismic events which cause visible damage to excavations, pose a threat to human population or interrupt mining activities are called rockbursts that are related to rock mechanics and geophysics. To monitor the state of the rock mass, knowing its response to the mining applied in presence of different hydrothermal bodies and the occurrence of large seismic events, the use of a spatial-temporal point process model called ETAS (Epidemic Type Aftershock Sequences) is proposed. The model simulates a process in which each event produces its own offspring events. To use this seismic indicator, it is necessary to determine parameters for a calibration period and establish an alert criterion σ called residual analysis, based on the difference between the measured and model-estimated seismicity. In order to implement the ETAS model in the future, calibration, evaluation, and application of parameters are discussed, based on the analysis of recorded seismicity during the construction of a tunnel in a mine located in Chile.

3. Methodology for the Seismic Alerts Standardization in Mining Using a Stochastic Model of Seismic Aftershocks

Fedilberto Gonzalez[a], Javier Vallejos[a,b]

[a] Advanced Mining Technology Center, University of Chile, Santiago, Chile

[b] Department of Mining Engineering, University of Chile, Santiago, Chile

Keywords: brittle behavior, seismic hazard, ETAS, residual analysis, AIC.

3.1. ABSTRACT

New Mine Level (NML) development tunnels have experienced brittle behavior and seismicity. Development blasts in the NML tunnels imply an increase of the seismic hazard generated by the possible violent release of energy in the predominant primary ore. These blasts generate seismic aftershocks clustered in space and time. To monitor the seismic response of the rock mass based on the space, time and magnitude of each seismic event recorded during the development of tunnel XC22/23, the stochastic ETAS (Epidemic Type Aftershock Sequences) model was proposed. The ETAS model simulates a process in which each event produces its offspring events, allowing the introduction of the concept of "induced" seismicity. By quantifying the difference between the measured and estimated seismicity with the model in terms of σ, it is possible to follow the seismic response of the rock mass in time. Some seismic alerts are given depending on a pre-established σ. Moreover, to implement the ETAS model in the future, calibration, evaluation according to Akaike selection criteria (AIC), and application of parameters are discussed.

3.2. INTRODUCTION

With the New Mine Level (NML) project, it is expected to increase the productivity of the El Teniente Mine. NML development tunnels have been carried out on primary ore and high-stress environments (Brzovic & Villaescusa, 2007). Due to changes in stresses resulting from mining excavations in these environments, NML tunnels have experienced brittle behavior and seismicity during their development (Brzovic et al., 2017; Rojas & Landeros, 2017). Below, a summary of the tunnels, magnitude of time according to Hanks-Kanamori moment magnitude and date of occurrence of the most relevant rockbursts during their development are exposed: (1) personal access tunnel developed by interior mining (TAP- M_w 2.5, Dec 2013); (2) personal access tunnel developed by exterior mining (P4600-M_w 1.2, Nov 2014); (3) ventilation tunnel developed by interior and exterior mining (XC22/23 - M_w 1.9, May 2015); (4) belt tunnel developed by exterior mining (TC - M_w 1.1, Mar 2018). To minimize employee losses or injuries as well as any loss in operational continuity due to induced seismicity, the stochastic modeling of mining induced seismicity ETAS (Epidemic Type Aftershock Sequences) model was proposed as a seismic indicator (Ogata, 1983; 1985; 1988; 1989; Zhou et al., 2018). The ETAS model allows to follow the response of the rock mass to the mining applied, based on the difference between the measured and estimated seismicity, a process that is called residual analysis (Trifu & Shumila, 2005; Vallejos, 2010). To illustrate the usefulness of the ETAS model, the seismicity recorded during the construction of a part of the XC22/23 ventilation tunnel was implemented. The analyzed tunnel is located at an altitude of 1876 m.a.s.l. and has an approximate overburden of 630 m. See Fig. 1 for illustration.

Figure 1. Main landscape features and mine sectors at the El Teniente Mine. Whole cross East- West section looking north showing the locations of major infrastructure tunnels. (from Rojas & Landeros 2017)

Based on the space, time and magnitude of each induced seismic event, it was possible to follow the response of the rock mass to the development blast by residual analysis in terms of σ. With a criterion of 1.5 standard deviations σ, several seismic events of large magnitude were alerted. Large events are considered as those with $M_w \geq 0.7$. Besides, the Akaike Selection Criteria (AIC) was implemented to evaluate the potential use of the ETAS model in real-time, namely, to calibrate a segment of the total period (Segment 1) and use its parameters in the remaining segment (Segment 2). Finally, it is perceived how the ETAS model through the residual analysis exhibits the seismic levels in the extension of the tunnel in the presence of three hydrothermal bodies A, B, and C, providing an understanding of the rock mass response to lithological changes.

In the next section, the model and methods for seismic activity analysis are presented. In section 2.4, the most important milestones of the construction of the tunnel XC22/23 are exhibited. Then, the model is implemented in the total period and analyzed parametrically along each of its segments. Finally, in order to evaluate the application of the methodology in future time periods, the model is calibrated in a segment of the total period, and when leaving its fixed parameters, it is applied in the remaining segment. Conclusions and some discussion are shown in section 2.5.

3.3. ETAS MODEL METHODOLOGY

The methodology used to evaluate the response of the rock mass to the applied mining consists of 5 stages (Gonzalez & Vallejos, 2019): (1) using a point process model to identify the measured seismic activity of the mining tunnel, defined by the historically dependent hazard rate, called the conditional intensity function. Based on the incorporation of well-established statistical laws for aftershocks, such as the Gutenberg-Richter magnitude frequency distribution and modified Omori law (Gutenberg & Richter, 1944; Ogata, 1992; Utsu et al., 1995); (2) estimation of the model's parameters using maximum likelihood in data sets over time $\{t_i\}_i^N$ and magnitudes $\{M_{wi}\}_i^N$ of occurrence in a period [S, T] in Eq. (4); (3) analysis of the relative performance of the model according to the selected data set using the Akaike information criterion (AIC) in the total period analyzed and two segments that make it up (Akaike, 1974); (4) analysis of the residual point process where ordinary time is nonlinearly changed based in Eq. (9); (5) quantification of the deviations between the measured seismicity and the one estimated by the model, applying a normal transformation to the residual (Shimizu & Yuasa, 1984; Ogata, 1988) evaluating the deviation in terms of the standard deviations σ (Ogata, 1992).

3.3.1. Epidemic-Type Aftershock-Sequences Model

The epidemic model ETAS (Epidemic Type Aftershock Sequences) proposed by Ogata (1988; 1989; 1999; 2001) simulates a process in which each seismic event has identical roles in the activation process, namely each seismic event produces its own offspring events. In this case, a seismic event occurring in time $\{t_i\}$ can generate an events rate that decay according to Omori's modified law (Utsu et al., 1995):

$$\boldsymbol{n(t) = \frac{K_i}{(c + t - t_i)^p}} \qquad \textbf{(1)}$$

Where c is a time compensation constant that considers the possible absence of seismicity recorded immediately after the main event, and p is a parameter proportional to the decay rate when p = 1 is the conventional Omori law (Omori, 1894; Trifu & Shumila, 2005). The frequency $n(t)$ in Eq. (1) can be considered as the conditional intensity function of a point process.

The epidemic model simulates a process in which K_i is proportional to the expected number of events whose magnitude exceeds a cut-off magnitude M_{wc} generated by an event of magnitude M_{wi}. The following form is proposed for K_i:

$$\boldsymbol{K_i = K_0 e^{\alpha(M_{wi} - M_{wc})}} \qquad \textbf{(2)}$$

where K_0 is a constant and α measures the effect of magnitude on the production of its own offspring events (Gospodinov & Rotondi, 2006). The model is given by the superposition of seismicity:

$$\boldsymbol{n_\theta(t) = \mu + \sum_{t_i<t} \frac{K_0 e^{\alpha(M_{wi} - M_{wc})}}{(c + t - t_i)^p}} \qquad \textbf{(3)}$$

The ETAS model described in Eq. (3) depends mainly on the occurrence times $\{t_i\}$ and magnitudes $\{M_{wi}\}$ of the seismic events before time t. The parameters μ, K, c, α, and p are estimates for several events in a given space of time. The μ parameter indicates the seismic background level, which means that the seismic events are normally recorded even without disturbances in the medium (Ogata, 1992). It is important to note that this seismic background level may change in the case of a large seismic event or disturbances around the excavation (Trifu & Shumila, 2005). As discussed by Vallejos (2010) the typical mining values for p and c range from 0.9 to 1.4 and 0.003 to 0.3 hours, respectively. The α parameter typically varies between 0.2 and 3.0, measuring the efficiency in which events above the magnitude M_{wc} generate sequences of events. Also, the α parameter is useful for quantitatively characterizing the seismicity type of a zone, allowing to gain knowledge of the possible seismic source. Typical seismic sequences in which there is an event of large magnitude and well-defined aftershocks that obey a decay in time according to Omori's law have an α parameter greater than 2.

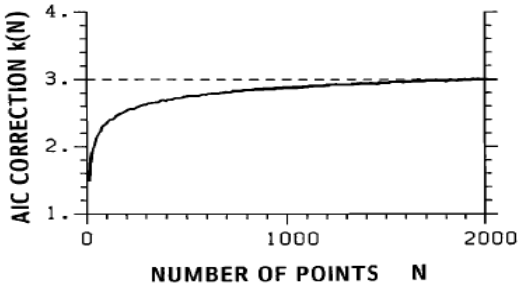

Figure 2. Penalty factor of the AIC for the change-point parameter. The Factor K(N) versus sample size N. (from Ogata, 1992)

3.3.2. Estimation of Model Parameters

To estimate the parameters of the model, it is important to make use of the maximum likelihood method. Given a parametric conditional intensity of seismicity $n_\theta(t \setminus H_t)$ with θ = (μ, K_0, c, α y p), depending on the history $H_t = (\{t_j\}_1^i, \{M_{wj}\}_1^i;\ t > t_i)$ of occurrence times and magnitudes, {i, j=1,2,…, N }of all events which occurred before t. For this, it is assumed that the distribution in the sequence of events is independent, and the likelihood function is determined (Ogata, 1992). The logarithm of this is given by:

$$\boldsymbol{logL\ (\theta; S; T) = \sum_{i=1}^{N} log\ n_\theta(t_i; H_t) - \int_S^T n_\theta(t; H_t)dt} \qquad \boldsymbol{(4)}$$

Where log is the logarithm, θ = (μ, K_0, c, α y p) presents the parameters to optimize, and $\{t_i; i = 1,2, \dots, N\}$, are the time $\{t_i\}_i^N$ with their respective magnitudes $\{M_{wi}\}_i^N$ of occurrence of the events in a time period [S, T], respectively.

For a rapid execution of the sequence model for aftershocks of epidemic type, the difference displayed in Eq. (4) was replaced by the forms of Eq. (5) and Eq. (6) (Ogata et al., 1993).

$$\sum_{i=1}^{N} \boldsymbol{log\ n_\theta(t_i; H_t)} = \sum_{i=1}^{N} \boldsymbol{log}\{\mu + \sum_{j=1}^{i-1} \frac{\boldsymbol{K_0 e^{\alpha(M_{wj} - M_{wc})}}}{\boldsymbol{(t_i - t_j + c)^p}}\} \qquad \boldsymbol{(5)}$$

$$\int_S^T \boldsymbol{n_\theta(t; H_t)dt} = \mu(\boldsymbol{T - S}) + \sum_{i=1}^{N} \int_0^{T-t_i} \frac{\boldsymbol{K_0 e^{\alpha(M_{wi} - M_{wc})}}}{\boldsymbol{(t + c)^p}} \boldsymbol{dt} \qquad \boldsymbol{(6)}$$

3.3.3. AIC Procedure

The maximum likelihood method allows to quantify the fit efficiency of the estimated models, namely, it allows the estimation of the relative performance at the model according to the selected data set. In this specific case, the same model is compared to 3 different scenarios: (1) the calibrated model over the complete database, that is, the total period; (2) the calibrated model for segment 1 based on the database of the total period; (3) the calibrated model with the remaining data from the total period data set, corresponding to segment 2. See Table 1 for the illustration. When implementing AIC, it is natural to have a measurement of the reproduction of the data set characteristics through simulations. As discussed by Akaike (1974), the best fit is obtained with the set of parameters having the lowest AIC value, given by:

$$\boldsymbol{AIC = -2 * max(ln(L\,(\theta;\, S;\, T)\,) + 2(num\ of\ parameters)} \qquad \textit{(7)}$$

ETAS model usually has five parameters to be adjusted, θ = (μ, K_0, c, α and p).

Before implementing the ETAS model in a future period, it had been confirmed that it was better to divide the total period [S, T] into the two proposed segments [S, T_0] and [T_0, T]. Therefore, the AIC was calculated for each proposed segment (AIC_1 and AIC_2) and compared with the AIC of the total period (AIC_0). The K(N) penalty is a parameter dependent on the number of events N in the intervals [S, T_0] and [T_0, T]. Fig. 2 illustrates the variation of the penalty factor K(N) in function of sample size.

$$\boldsymbol{AIC_0 = (-2)\,max\,ln\,L((\theta;0,\,T) + 2x5)}$$
$$\boldsymbol{AIC_{12} = AIC_1 + AIC_2 + 2k(N)}$$
$$\boldsymbol{AIC_1 = (-2)\,max\,ln\,L((\theta;0,\,T0) + 2x5)}$$
$$\boldsymbol{AIC_2 = (-2)\,max\,ln\,L\,((\theta;\,T0,T1) + 2x5)}$$

$AIC_{12} < AIC_0$ indicates a significant distinction between the seismicity patterns in the two divided periods. Therefore, having parameters for each space-time will be more representative than the total period. Consequently, it will be more representative to use the period parameters [S, T_0] to reproduce the seismic response of the period rock mass [T_0, T]. An example of the application of the ETAS model parameters in real-time is illustrated in section 3.3.

3.3.4. Residual Analysis

To use the ETAS model as a seismic indicator, it is necessary to determine the associated parameters and establish an alert criterion based on the difference between the measured seismicity and the one estimated by the model, which is called residual analysis (Ogata, 1988; 1989; 1999; 2001). This method consists of transforming real time in a non-linear manner based on the integration of the estimated seismicity occurrence rate by the model. The transformed time is given by:

$$\boldsymbol{A_\tau = \int_S^t n_\theta\,(t; H_t)dt} \qquad \textit{(8)}$$

The transformed time corresponds to the number of seismic events estimated by the model for an interval [S,t_j] as can be seen in Fig. 3. The Eq. (9) represents an increasing function, which considers the change over time of $\tau_i = A_{t_i}$. Then, the times $\{t_i\}$ are transformed 1 to 1 in $\{\tau_i\}$, a transformation that is called the Residual Point Process (RPP) (Ogata, 1992).

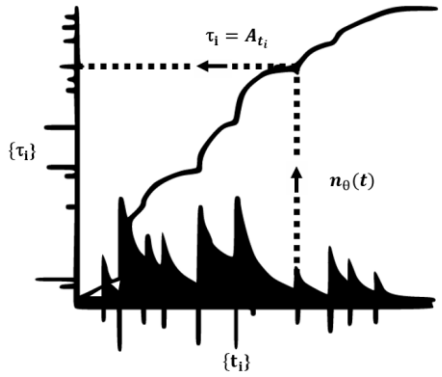

Figure 3. A schematic diagram of the time transformation of original events into RPP events. (from Ogata, 1992)

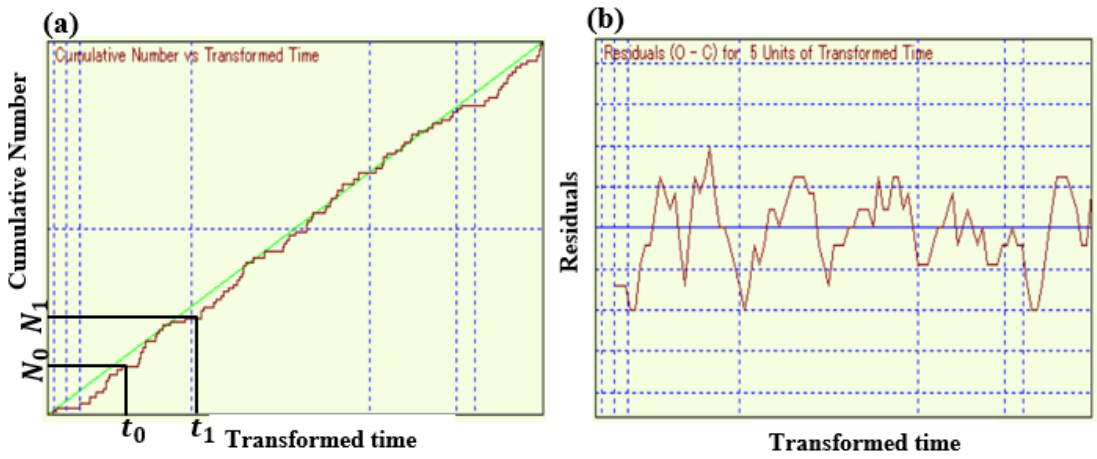

Figure 4. Example of residual analysis with ETAS model. (a) Cumulative number of events as a function of transformed time, (b) Residuals as a function of transformed time (from Ogata, 1988;1989)

$$\tau_j = \int_S^{t_j} \mu + \sum_{t_i<t_j} \frac{K_0 e^{\alpha(M_{wi}-M_{wc})}}{(c+t_j-t_i)^p} dt \qquad (9)$$

As discussed by Ogata (1992), some authors such as Lomnitz (1982) and Lomnitz & Nava (1983) have questioned the usefulness of the deviation between the measured seismic rate and the one estimated by the ETAS model as an alert criterion. They argue that it can be a mere effect of the decadent activity of the aftershocks of the last large seismic event or disturbance in the environment. However, according to Ogata (1992), this option can be easily ruled out because transformed times or RPP data are implemented in the seismicity analysis obtained from Eq. (8) with Eq. (3) by modeling the aftershock effect. See Eq. (9) for the illustration.

To quantify the deviations of the measured seismic rate from that estimated by the ETAS model, it is necessary to apply a transformation of variables in such a way that the residual approximates a normal distribution with a mean of 0 and a variance of 1. However, before carrying out this process, it is necessary to establish a fixed transformed time interval h, which estimates the number of real events that occurred in that period.

Fig. 4 presents an example of an estimation of the residuals between the number of events measured and estimated by the ETAS model for a transformed time interval $[\tau_0, \tau_1]$ by means of the application developed by Ogata (1988; 1989). Given a fixed transformed time interval h = $\tau_1 - \tau_0$ the number of actual events occurring in that interval is estimated $\Delta N_1 = N_1 - N_0$. The residual for this interval is given by R = $\Delta N - h$.

The transformation of variables is given by Shimizu & Yuasa (1984):

$$\chi_i(\Delta N_i, h) = \frac{33\Delta N_i + 29 - h - (32\Delta N_i + 31)[\frac{h}{\Delta N_i} + 1]^{\frac{1}{4}}}{(9\Delta N_i + 1)^{\frac{1}{2}}} \qquad (10)$$

Based on Eq. (10) it is possible to evaluate the degree of deviation between the measured seismicity and that estimated by the model in terms of the standard deviation σ of the normal distribution.

3.4. RESULTS

This section consists of 3 stages: (1) Fig. 5 represents a timeline display with the most relevant events associated with the construction of the tunnel XC22/23 mentioned in section 1; (2) calibration and analysis

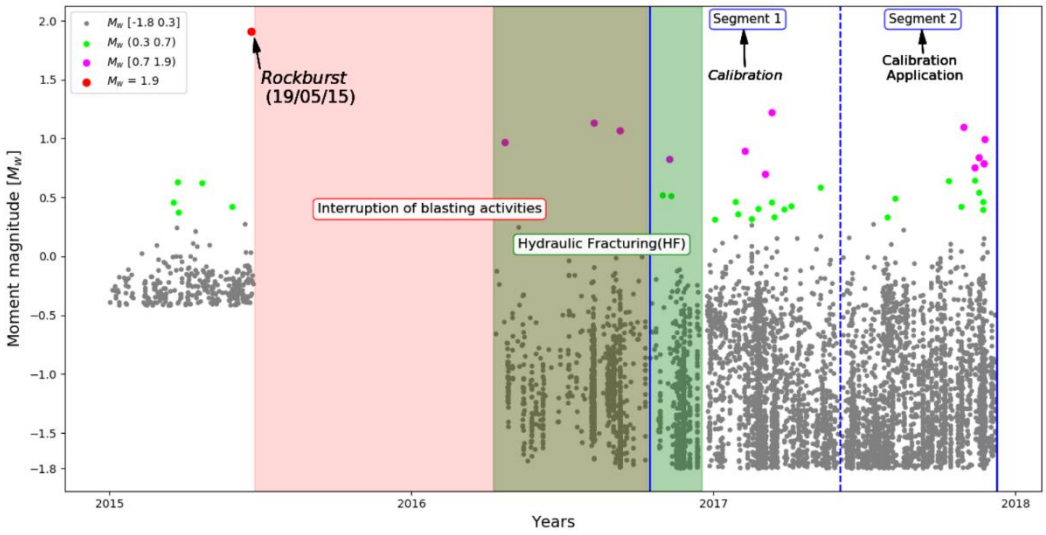

Figure 5. Timeline of most relevant events in the construction of the tunnel. Real-time seismicity with magnitudes as proposed by Hudyma et al. (1995); Occurrence of rockburst; Interruption of blasting activities in red; Implementation of pre-conditioning (HF) in green; Total period implemented for analysis of the methodology; Segment 1 of the total period implemented for calibration; Segment 2 of the total period, implemented for calibration and application, leaving the parameters of segment 1 fixed

of the model parameters for the total period and its two segments; (3) application of the ETAS methodology in segment 2, with the fixed parameters of segment 1, the residuals are analyzed and interpreted for a future period in connection with events of large magnitude.

Table 1. Seismicity subsets employed in this study

Subset	Time Interval (dd/mm/yy)	M_{wc}	N
Total period	22/09/16 - 06/12/17	-1.8	4,490
Segment 1	22/09/16 - 01/05/17	-1.8	2,222
Segment 2	02/05/17 - 06/12/17	-1.8	2,268

3.4.1. Milestone

The completeness magnitude (M_{wc}) corresponds to the minimum magnitude that the seismic network can record. The intervals of time, the number of seismic events N and the M_{wc} by which the applicability of the previous model to the evaluation of the seismic hazard in the construction of the tunnel is verified are shown in Table 1, where no specific criteria for the selection of its segments are considered.

The construction of this tunnel was successfully completed on December 7, 2017 and has an extension of approximately 442 meters. This excavation was abruptly interrupted in May 2015 due to the occurrence of a rockburst of M_w 1.9 and energy $5.2*10^7$[J], causing severe damage along 150 meters approximately. Since the occurrence of this rockburst, the decision to improve the sensitivity of the seismic monitoring network varying from M_{wc} -0.7 to M_{wc} -1.8 was taken. In addition, between March and December 2016, the HF was carried out in 11 wells to reduce the seismic hazard of the sector. The blasting operations were resumed in September 2016 after their interruption that occurred in May 2015. See Fig. 5 for the illustration.

3.4.2. Calibration and Analysis of the Model Parameters

The black line in graphs (b) in Figs. 6–9 represents the residual analysis of the analyzed periods according to Eq. 10. However, the remaining graphs (a), (c), (d), and (e) are complementary for understanding fully the changes in seismic levels. These graphs are called "auxiliary" because they support the interpretation of the residuals in the main graph (b). For simplicity, only the caption for Fig. 6 contains the explanation that applies to Figs. 6–9.

The tops of the figures mentioned above show the application dates of the ETAS model. The bottoms show the completeness magnitude (M_{wc}), the developed meters (d.m.) with a certain number of blasts (N.B.) in the analysed period were estimated together with the ETAS model parameters and their respective AICs according to Eq. 7. The k(N) penalty was used to identify changes in seismicity patterns in the proposed periods. The blue dotted vertical lines indicate the presence of events with large magnitudes (L.M.). Table 2 presents a summary of the parameters mentioned above, both for the calibration parameters and those for application, including the k(N) penalty.

In this research, it was possible to illustrate the change of residual behaviour according to lithological changes and tunnel advancement rate. Therefore, the importance of the estimated fixed transformed time *h* in calibration is highlighted here. Empirically, the best interpretations of the residual were achieved with an *h* between 1/10 and 1/15 of *N* for the adjustment.

In Figs. 6–9, graph (a) represents the number–size cumulative event distributions for the subsets in Table 2. This graph is the only one that shows real-time results; the remaining graphs are functions of the transformed times. The yellow, cyan, and red colours presented in graph (b) for each figure correspond to the hydrothermal bodies A, B, and, C recognised by geology, respectively. The figures are presented with respect to time while hydrothermal bodies have spatial characteristics. The duration of time of

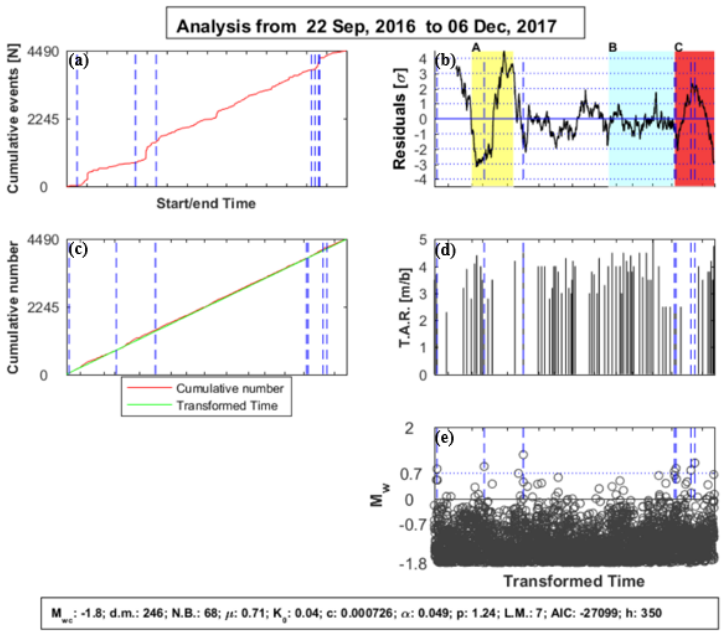

Figure 6. The response of the rock mass to the mining applied including calibration of the total period. Ticks on the x-axis of this graph denote months while the start date is shown in the top section of the figure. (a) Cumulative events as a function of real time, (b) residuals as a function of transformed time, (c) cumulative number of events and estimated number of events (in red and green, respectively) according to the ETAS model by means of Eq. 9 as functions of transformed time, (d) tunnel advance rate as a function of transformed time, and (e) occurrence of seismic events as a function of transformed time

mining/development through the bodies allows the relation between space and time to be identified. Based on this graph, the alert criterion is defined. After defining the time interval h, the period analysed is divided into intervals of h size to estimate the degree of deviation between the measured and model seismicity in terms of the standard error of a normal distribution according to Eq. 10. Finally, the expert in charge of the process defines the standard error σ used to notify as to whether the indicator is in an alert state or not, i.e. when $|\chi_i(\Delta N_i, h)| \geq \sigma$.

Being in a state of seismic alert does not ensure the occurrence of large seismic events. Rather, a state of seismic alert reports that the seismic response of the rock mass does not meet expectations, increasing the possibility of an event of large magnitude and, at the same time, the frequency of false alarms. Considering that extractive activities, blasts, and lithological changes are not continuous in space and time, it is logical that the number of false alarms tends to increase over time. Much work remains to be done before rock bursts can be anticipated. It is hoped that the present research helps contribute to the understanding of this complex phenomenon (Manouchehrian & Cai 2018).

Graph (c) in each of Figs. 6–9 visualizes the accumulated number of real and estimated events according to the ETAS model using Eq. 9 as a function of time transformed into red and green, respectively. Graph (d) shows the tunnel advance rate (T.A.R.) and the advance blasting performed for the period considered, quantifying its advance in meters per blasting event $[\frac{m}{b}]$. Graph (d) shows that development blasting, inherent to the mining cycle, may be the main cause of large seismic events. It is important to emphasise that not every blasting event triggers large-magnitude events. On the other hand, graph (e) visualises the presentation of seismic events in transformed time, helping to understand the fluctuations in the residual of (b).

Figure 6 shows the response of the rock mass to the mining applied during the total period. In graph (b) of this figure, seven large-magnitude seismic events occurred, indicated by the vertical blue dotted lines. The first occurred during the first interval h, where there was no residual. The second, third, fifth, sixth, and seventh large events occurred when the deviation σ indicated that the system was in a state of seismic alert. Finally, the fourth event of large magnitude occurred in the transition between the B and C hydrothermal bodies.

There are two possible types of rock bursts described by Feng et al. (2017), classified according to their time of occurrence after a disturbance in the tunnel: immediate and time-delayed rock bursts. The sixth and seventh large events in Fig. 6 are of the time-delayed type and were alerted using the ETAS approach. The

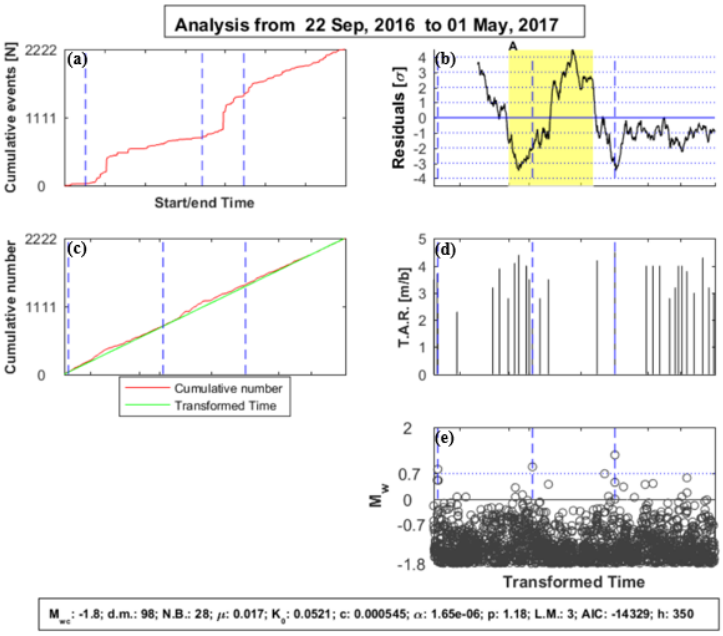

Figure 7. The response of the rock mass to the mining applied. Calibration of segment 1 of the total period

remaining large-magnitude events are illustrated through auxiliary graphs and were of the immediate rock burst type, as in the case of (d). The date of blasting is important in classifying rock bursts according to their type.

Another application of residual analysis is to determine the response of a rock mass to changes in lithology (A, B, and C), classifying these hydrothermal bodies according to the seismic hazards they pose. During mining applied to hydrothermal body A, the ETAS model allowed alerting of the occurrence of an event of large magnitude. Moreover, graph (b) in Fig. 6 illustrates the instability of the seismic levels in the presence of this hydrothermal body. Hydrothermal body B presents the most stable seismic levels as a response to applied mining. Finally, during the mining activities on hydrothermal body C, four large-magnitude seismic events occurred, which makes this hydrothermal body the one with the most significant seismic hazard.

The occurrence of large-magnitude events and the analysis of development blasting increased the background level μ. The α parameter indicated that larger-magnitude events in the catalogue for the calibration segment did not generate seismic sequences with a well-defined decay in time of the type described by Omori's law. The p parameter found by Eq. 3 was within the range estimated for other mines, as discussed by Vallejos (2010). The swarm-type seismicity represented by the α parameter could increase the speed of decay p. On the other hand, the AIC indicated that the approach presented a satisfactory fit with the implemented database. This is illustrated in Table 2.

Figure 7 shows the response of the rock mass to the mining applied during segment 1. In graph (b) of this figure, three large-magnitude seismic events occurred, indicated by the vertical blue dotted lines. The first occurred during the first interval h, where there was no residual. The second and third large-magnitude events occurred when the deviation σ indicated that the system was in a state of seismic alert. These large-magnitude events were of the immediate rock burst type.

The α and p parameters found in segment 1 were marginally different from those reported for the analysis of the total period. The decrease in background levels of segment 1 compared to the total period and segment 2 could have been due to the lower number of development blasting events. The AIC, though higher than in the total period, indicated that the approach presented a satisfactory fit with the implemented database.

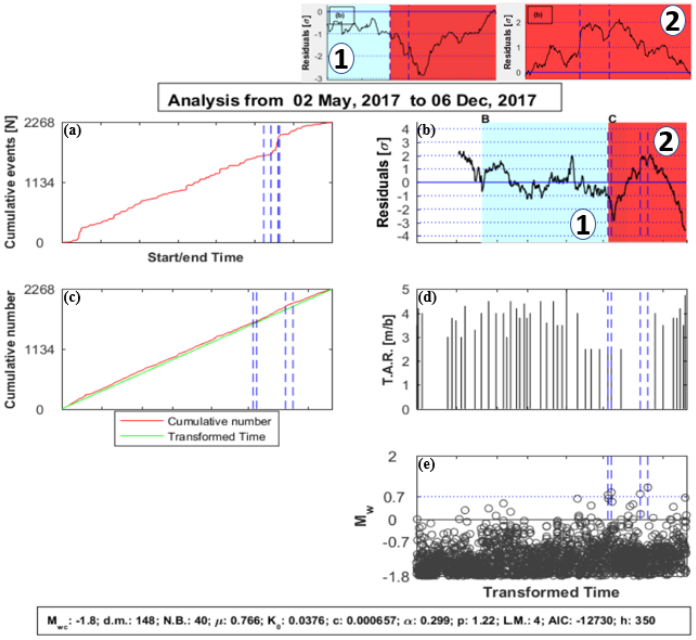

Figure 8. The response of the rock mass to the mining applied. Calibration of segment 2 of the total period

Figure 8 shows the response of the rock mass to the mining applied during segment 2. In graph (b) of this figure, four large-magnitude seismic events occurred, indicated by the vertical blue dotted lines. The first large-magnitude event belonged to the immediate rock burst type. The three remaining large seismic events occurred when the deviation σ indicated that the system was in a state of seismic alert. It is important to note that the first large-magnitude events occurred during the transition between the B and C hydrothermal bodies, a possible cause being the change in intrinsic stiffness of each lithology.

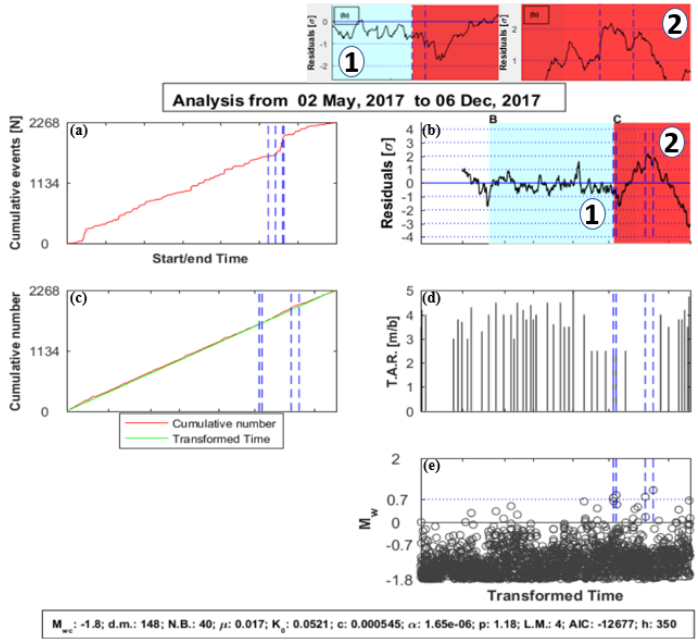

Figure 9. Response of the rock mass to the mining applied. Application of the model in segment 2, leaving the parameters of segment 1 fixed, analysis in real time.

Table 2. Evaluation of the seismic response in calibration and application for the XC22/23 tunnel

Parameter	Total Period	Segment 1	Segment 2	Period 2 Application
Time Interval (dd/mm/yy)	22/09/16 - 06/12/17	22/09/16 - 01/05/17	02/05/17 - 06/12/17	02/05/17 - 06/12/17
M_{wc}	-1.8	-1.8	-1.8	-1.8
N.B.	68	28	40	40
d.m.	246	98	148	148
N	4,490	2,220	2,270	2,270
μ	0.7	0.02	0.8	0.02
K_o	0.04	0.05	0.04	0.05
C	7×10^{-4}	6×10^{-4}	7×10^{-4}	6×10^{-4}
P	1.24	1.18	1.2	1.18
α	0.049	$0.016\text{x}10^{-4}$	0.30	$0.016\text{x}10^{-4}$
2K(*N*)		6.0	6.0	
AIC	-27,099	-14,323	-12,724	-12, 677

The α parameter was greater for the analysis corresponding to Fig. 8 than that corresponding to Figs. 6 and 7. On the other hand, the μ parameter was greater for the analysis of Fig. 8 than Fig. 7 and marginally different from Fig. 6. The increase in μ was due to the larger number of blasts during segment 2. The increase of the α parameter indicated an increase in seismic hazard. The α and p parameter values were consistent with the largest number of development blasting events in segment 2. The AIC, though higher than in the total period, indicates that the approach presented a satisfactory fit with the implemented database.

Although parameter variability was low over the segments analysed and over the total period, it was necessary to evaluate a possible change in seismicity patterns and, consequently, to use the parameters found when applying the ETAS model to a future period. Therefore, compared with the AIC of the total period (AIC_T), those of segments 1 (AIC_1) and 2 (AIC_2) were penalised by the *K* factor according to their respective *N* values. According to Table 2, as AIC_T (-27,099) < AIC_{12} (-27,047), it was better to adopt values obtained for the total period; this caused no significant changes in seismicity patterns.

Table 3. Results presented by Trifu & Shumila (2005)

Subset	Kidd 1	Kidd 2	Creighton 1	Creighton 2	Darlot 1	Darlot 2
Time Interval (dd/mm/yy)	01/09/02 - 31/11/02	01/12/02 - 10/04/03	09/09/02 - 31/11/02	05/01/03 - 31/01/03	01/09/03 - 31/12/03	01/10/03 - 29/04/04
M_{wc}	-1.9	-1.8	-2.0	-2.0	-1.3	-1.4
N	1,522	4,155	9,910	7,785	1,358	2,986
μ	0.001	0.004	0.03	0.01	0.001	0.001
K_o	0.47	0.50	5.89	0.81	0.73	0.60
c	6.0×10^{-3}	5.0×10^{-3}	3.0×10^{-3}	1.0×10^{-3}	4.0×10^{-3}	3.0×10^{-3}
p	1.74	1.37	1.00	1.01	1.58	1.48
α	0.82	0.78	0.92	1.58	0.00020	0.16

3.4.3. Application of Parameters at Future Times

Parameters recommended by the AIC must be used in a future period. Since segment 2 fell within the parametric calibration of the total period, it is expected that the residuals show satisfactory behaviour when applying the parameters. Therefore, to achieve real-time application, the parameters of segment 1 were fixed and implemented in segment 2. Figure 9 shows the response of the rock mass to the mining applied during the segment 2 period using the parameters fixed from segment 1. The response of the rock mass to mining applied to the B and C hydrothermal bodies illustrated in graph (b) in Figs. 8 and 9 was similar. The second and third events of large magnitude raised alerts during calibration and not in application. However, large-magnitude seismic events for the time-delayed rock burst type occurred during mining of the hydrothermal body when the system entered a state of seismic alert.

According to Table 2, the AIC value (-12,730) in calibration was similar to the AIC value (-12,677) in application. Therefore, the results of implementing the ETAS model to a future period were satisfactory. It is advisable to replicate this research in order to verify these conclusions with different study cases.

3.5. CONCLUSIONS

For the evaluation of the seismic hazard in mining, it is necessary to understand the generation of seismic events from both the main event and the dependent events. Therefore, it is important to implement the ETAS model, which simulates a process in which each event produces its own offspring events. After fitting the ETAS model to the maximum likelihood occurrence data, it is possible to estimate the expected occurrence rate of seismic events. To use this model as a seismic indicator, it is necessary to compare the expected rate with the rate of occurrence of seismic events, a process called residual analysis.

The causality in the generation of seismic events exhibited by the ETAS model through the residual analysis is useful to compare the response of the rock mass to the applied mining during the presence of different hydrothermal bodies. Under the premise that each hydrothermal body has a different stiffness modulus, it is possible to classify them according to the historical seismic hazard in case of a future appearance in the excavations. See Fig. 6 for the illustration.

The parameters of the ETAS model are affected by the mining process. It is recommended to use the best fit time period of records to calibrate the parameters. Therefore, it is suggested to divide the periods according to AIC. Finally, an adequate reading of the ETAS model parameters found in the total period and each of its segments by means of maximum likelihood is key to the interpretation of the response of the rock mass to the applied mining.

In previous work, Trifu & Shumila (2005) implemented the α parameter to represent the seismic hazard of mines in Canada and Australia. Table 3 presents a summary of the results of the ETAS model applied in the Kidd and Creighton mines in Ontario and at the Darlot mine in Western Australia. The lower seismic hazard in these mines was associated with lower values of the α parameter because seismic aftershocks tend to die out. This research implements the approach proposed by Trifu & Shumila (2005) to represent the seismic hazard with the α parameter. The low value of α parameter in the three analyses performed according to Table 2, indicates that the largest events in the catalog do not generate seismic sequences with a well-defined decay in time of the type described by Omori's law. This can be attributed to the HF carried out between March-December 2016 if we consider that the fractured rock has less capacity to store energy due to its capacity to dampen high stresses within the cracks (Feng et al.,2017). To confirm this hypothesis, it is advisable to replicate this work in another tunnel of the same mine, ensuring greater geological similarity and, at the same time, a less biased comparison.

The available information about the execution time and advance of each blast is useful for classifying rockburst as proposed by Feng et al., (2017). However, to quantify the energy supplied to the rock mass, it is recommended to include the amount of explosive implemented in each blast, allowing to analyze the response of the residuals in graphs (b) of Figs. 6-9 more accurately and complementing graph (d). The auxiliary graphics (a), (c), (d) and (e) in the figures mentioned above, allow a synergy that favors the justification of the residuals in (b).

3.6. ACKNOWLEDGEMENTS

The authors gratefully acknowledge the financial support from basal CONICYT project AFB180004 of Advanced Mining Technology Center (AMTC)- University of Chile. In addition, I would like to take this opportunity to thank Dr. Dmitriy Malovichko for reading and helping me improve this article.

3.7. REFERENCES

Akaike, H. (1974). A new look at the statistical model identification. IEEE transactions on automatic control, 19(6), 716–723. https://doi.org/10.1109/TAC.1974.1100705.

Brzovic Skarmeta, J, Blanco, B, Dunlop, R, Sepulveda, MPA. (2017). Sub-horizontal faulting mechanism for large rockbursts at the El Teniente mine. In: The 9th Rockburst and Seismicity in Mines Symposium (RaSIM 9).

Brzovic, A., & Villaescusa, E. (2007). Rock mass characterization and assessment of block-forming geological discontinuities during caving of primary copper ore at the El Teniente mine, Chile. International journal of rock mechanics and mining sciences, 44(4), 565-583.

Feng, X. T., Chen, B. R., Feng, G., Zhao, Z., Zheng, H., & Al Heib, M. (2017). Description and engineering phenomenon of rockbursts. Rockburst: mechanisms, monitoring, warning, and mitigation, 3–26. https://doi.org/10.1016/B978-0-12-805054-5.00001-9.

Gonzalez, F. J., and J. A. Vallejos. (2019). Evaluation of the Seismic Response of the Rock Mass Using a Model of Seismic Aftershocks of the Epidemic Type. 53rd US Rock Mechanics/Geomechanics Symposium. American Rock Mechanics Association.

Gospodinov, D., & Rotondi, R. (2006). Statistical analysis of triggered seismicity in the Kresna region of SW Bulgaria (1904) and the Umbria-Marche region of central Italy (1997). Pure and applied geophysics, 163(9), 1597–1615. https://doi.org/10.1007/s00024-006-0084-4.

Gutenberg R, Richter CF. (1944). Frequency of earthquakes in California. Bull Setstool Soc Am 3:185–188.

Hudyma, M. R., Milne, D., & Grant, D. R. (1995). Geomechanics of sill pillar mining in rockburst prone conditions. Final report: sill pillar monitoring using conventional methods. Mining research directorate.

Lomnitz C. (1982). What is a Gap? Bull Seism Soc Am 7:1411–1413.

Lomnitz C, Nava, FA. (1983). The predictive value of seismic gaps. Bull Seism Soc Am 73:1815–1824Manouchehrian, A., & Cai, M. (2018). Numerical modeling of rockburst near fault zones in deep tunnels. Tunnelling and Underground Space Technology, 80, 164-180.

Manouchehrian A, Cai M (2018) Numerical modeling of rockburst near fault zones in deep tunnels. Tunn Undergr Sp Technol 80:164–180. https://doi.org/10.1016/j.tust.2018.06.015

Ogata, Y.(1983). Estimation of the parameters in the modified Omori formula for aftershock frequencies by the maximum likelihood procedure, J. Phys. Earth, 31, 115-124.

Ogata, Y. (1985). Statistical models for earthquake occurrences and residual analysis for point processes, Res. Memo. (Technical report) 288, Inst. Statist. Math., Tokyo, 1985.

Ogata, Y. (1988). Statistical models for earthquake occurrences and residual analysis for point processes. Journal of the American Statistical Association, 83(401), 9–27. https://doi.org/10.1080/01621459.1988.10478560.

Ogata Y. (1989). Statistical model for standard seismicity and detection of anomalies by residual analysis. Tectonophysics 169:159–174. https://doi.org/10.1016/0040-1951(89)90191-1.

Ogata Y. (1992). Detection of precursory relative quiescence before great earthquakes through a statistical model. J Geophys Res 97:19845. https://doi.org/10.1029/92jb00708.

Ogata Y, Matsu'ura RS, Katsura K. (1993). Fast likelihood computation of epidemic type aftershock-sequence model. Geophys Res Lett 20:2143–2146. https://doi.org/10.1029/93gl02142.

Ogata, Y. (1999). Seismicity analysis through point-process modeling: A review. Pure and applied Geophysics, 155(2–4), 471–507. https://doi.org/10.1007/s000240050275.

Ogata, Y. (2001). Increased probability of large earthquakes near aftershock regions with relative quiescence Yosihiko. Geophysics, 106, 8729–8744.

Omori, F. (1894). On the after-shocks of earthquakes. The Journal of the College of Science, Imperial University of Tokyo, 7, 111-200.

Rojas E, Landeros P. (2017). Hydraulic fracturing applied to tunnels development at El Teniente mine. In: The 9th Rockburst and Seismicity in Mines Symposium (RaSIM 9).

Shimizu, R., & Yuasa, M. (1984). Normal approximation for asymmetric distributions. Proc. Inst. Stat. Math, 32, 141-158.

Trifu, C., & Shumila, V. (2005). Seismic hazard assessment in mines using a marked spatio-temporal point process model. Controlling Seismic Risk (Eds. Potvin, Y., and Hudyma, M.), Australian Centre for Geomechanics, Perth, Australia, 461–467.

Utsu T, Ogata Y, Matsu'ura R. (1995). The Centenary of the Omori Formula for a Decay Law of Aftershock Activity. J Phys Earth 43:1–33. https://doi.org/10.4294/jpe1952.43.1

Vallejos, J. A. (2010). Analysis of seismicity in mines and development of re-entry protocols by, 403.

Zhou, J., Li, X., & Mitri, H. S. (2018). Evaluation method of rockburst: state-of-the-art literature review. Tunnelling and Underground Space Technology, 81, 632-659.

4. CONCLUSIONES GENERALES

Para evaluar el peligro sísmico en minería, es necesario entender la generación de eventos sísmicos a partir del evento principal y de los eventos dependientes. Por lo tanto, es apropiado implementar el modelo ETAS, que simula un proceso en el que cada evento produce sus propios eventos descendientes.

Una lectura adecuada de los parámetros del modelo ETAS encontrados en el período total, y cada uno de sus segmentos utilizando la máxima verosimilitud, es crítica para la interpretación de la respuesta del macizo rocoso a la minería aplicada. Los parámetros del modelo ETAS se ven afectados por el proceso minero. Se recomienda utilizar el período de ajuste óptimo de los registros para calibrar los parámetros.

Los gráficos auxiliares (a), (c), (d), y (e) de las Figuras del artículo expuesto, permiten entender el comportamiento de los residuales en (b).

El análisis residual presenta valores más altos antes de que ocurran algunos de los eventos de gran magnitud. Los valores residuales no parecen verse afectados significativamente por la utilización de los parámetros de los distintos períodos. Existe una diferencia marginal entre el AIC del período de calibración y el período de aplicación.

Estar en estado de alerta sísmica no asegura la ocurrencia de grandes eventos sísmicos. Sin embargo, un estado de alerta sísmica reporta que la respuesta sísmica del macizo rocoso no cumple con nuestras expectativas, aumentando la posibilidad de que ocurra un evento de gran magnitud y al mismo tiempo, la cantidad de falsas alarmas.

Considerando que las actividades extractivas, voladuras y cambios litológicos no son continuos en el espacio y el tiempo, es lógico que el número de falsas alarmas tienda a aumentar. Todavía queda un largo camino por recorrer antes de que podamos predecir los rockbursts. Se espera que sea posible contribuir a la comprensión de este fenómeno complejo.

Los parámetros del modelo ETAS podrían utilizarse para cuantificar el impacto del pre-acondicionamiento en la respuesta sísmica del macizo rocoso a la minería aplicada. El peligro sísmico podría ser cuantificado a través del parámetro α. Se analizarán y publicarán más casos.

5. RECOMMENDACIONES Y TRABAJO FUTURO

Considerando que la sismicidad en las minas es inducida por cambios de esfuerzos antropogénicos en el macizo rocoso, los eventos sísmicos "descendientes" pueden ser producidos no sólo por otros eventos sísmicos de mayor envergadura, sino también por cambios de esfuerzos impuestos dentro del macizo rocoso. El efecto de este último puede describirse agregando un término en la Eq. (3), que depende del nivel de los cambios de esfuerzo impuesto o de su equivalente (por ejemplo, el volumen minado o la cantidad de explosivo implementado por cada voladura).

Es importante analizar tanto la disminución como el aumento de la actividad sísmica estimada con el modelo ETAS. Ambos casos tienen un alto peligro sísmico inherente.

Los resultados deben ser correlacionados con el proceso de minería. Por lo tanto, se sugiere dividir los períodos según el AIC.

Para obtener resultados más precisos con el modelo ETAS, se recomienda maximizar el N durante la calibración de parámetros.

En trabajos futuros, se recomienda replicar esta metodología en diferentes túneles de la mina El Teniente. La implementación del modelo ETAS en catálogos sísmicos de macizos rocosos preacondicionados con fracturamiento hidráulico y destressing permitiría comparar los efectos de estas técnicas. En este sentido, sería posible conocer el efecto real del preacondicionamiento sobre la generación de réplicas sísmicas, la velocidad de decaimiento y, en consecuencia, el peligro sísmico.